JOURNAL OF NATURAL PRODUCTS

pubs.acs.org/jnp

Article

# Identification of Biosynthetic and Metabolic Genes of 2-Azahypoxanthine in *Lepista sordida* Based on Transcriptomic Analysis

Mihaya Kotajima, Jae-Hoon Choi,* Hyogo Suzuki, Tomohiro Suzuki, Jing Wu, Hirofumi Hirai, David C. Nelson, Hitoshi Ouchi, Makoto Inai, Hideo Dohra, and Hirokazu Kawagishi*

Cite This: https://doi.org/10.1021/acs.jnatprod.2c00789

Read Online

ACCESS | Metrics & More | Article Recommendations | Supporting Information

**ABSTRACT:** 2-Azahypoxanthine was isolated from the fairy ring-forming fungus *Lepista sordida* as a fairy ring-inducing compound. 2-Azahypoxanthine has an unprecedented 1,2,3-triazine moiety, and its biosynthetic pathway is unknown. The biosynthetic genes for 2-azahypoxanthine formation in *L. sordida* were predicted by a differential gene expression analysis using MiSeq. The results revealed that several genes in the purine and histidine metabolic pathways and the arginine biosynthetic pathway are involved in the biosynthesis of 2-azahypoxanthine. Furthermore, nitric oxide (NO) was produced by recombinant NO synthase 5 (rNOS5), suggesting that NOS5 can be the enzyme involved in the formation of 1,2,3-triazine. The gene encoding hypoxanthine-guanine phosphoribosyltransferase (HGPRT), one of the major phosphoribosyltransferases of purine metabolism, increased when 2-azahypoxanthine content was the highest. Therefore, we hypothesized that HGPRT might catalyze a reversible reaction between 2-azahypoxanthine and 2-azahypoxanthine-ribonucleotide. We proved the endogenous existence of 2-azahypoxanthine-ribonucleotide in *L. sordida* mycelia by LC-MS/MS for the first time. Furthermore, it was shown that recombinant HGPRT catalyzed reversible interconversion between 2-azahypoxanthine and 2-azahypoxanthine-ribonucleotide. These findings demonstrate that HGPRT can be involved in the biosynthesis of 2-azahypoxanthine via 2-azahypoxanthine-ribonucleotide generated by NOS5.

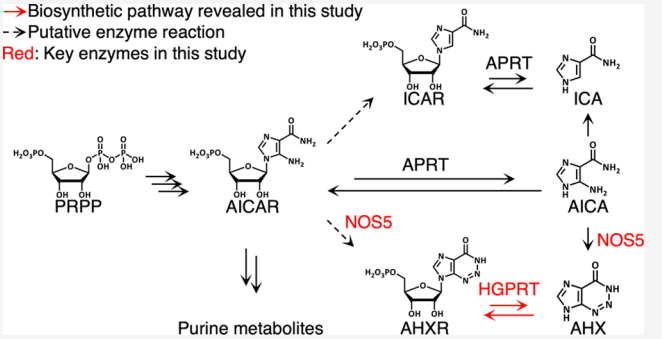




"Fairy rings" are naturally occurring ring- or arc-shaped clusters of mushrooms that are formed by about 60 species of fungi in soil. In turfgrass, these rings are often preceded by the appearance of vigorous plant growth or plant death,[1−7] which suggests that fairy ring-forming fungi may produce plant growth regulators. Two such compounds, 2-azahypoxanthine (AHX) and imidazole-4-carboxamide (ICA), were isolated from the culture broth of *Lepista sordida*, which is one of the major fairy ring-forming fungi. 2-Aza-8-oxohypoxanthine (AOH) was subsequently found in rice plants treated with 2-azahypoxanthine.[8−11] These compounds are collectively referred to as "fairy chemicals" (FCs).[12] Fairy chemicals show growth-regulating activity toward not only turfgrass but also various plants.[9−11] Fairy chemicals increase the yields of crops such as wheat and rice in greenhouse and/or field experiments.[9−11,13−15] Fairy chemicals also enhance tolerance to abiotic stress, supporting their potential utility in agriculture.[9−11]

The molecular mechanisms by which fairy chemicals influence plant growth are not yet known, but progress has been made toward understanding the metabolism of these compounds (Figure 1). Fairy chemicals are endogenously produced by plants as well as fungi such as *L. sordida*.[6,7,16] 5-Aminoimidazole-4-carboxamide (AICA) is a compound of the purine metabolic pathway that is common to microorganisms, plants, and animals. Metabolic labeling experiments with double-$^{13}$C-labeled 5-aminoimidazole-4-carboxamide have shown that 5-aminoimidazole-4-carboxamide is converted into fairy chemicals in *L. sordida* (Figure 1). Supporting this, the addition of 5-aminoimidazole-4-carboxamide-1-$\beta$-D-ribofuranosyl 5′-monophosphate (AICAR), a phosphoribosylated precursor of 5-aminoimidazole-4-carboxamide in the purine pathway, to mycelial culture results in increased 2-azahypoxanthine abundance.[16,17]

2-Azahypoxanthine and its derivative 2-aza-8-oxohypoxanthine feature an unusual 1,2,3-triazine moiety. Recently, we

**Received:** September 5, 2022

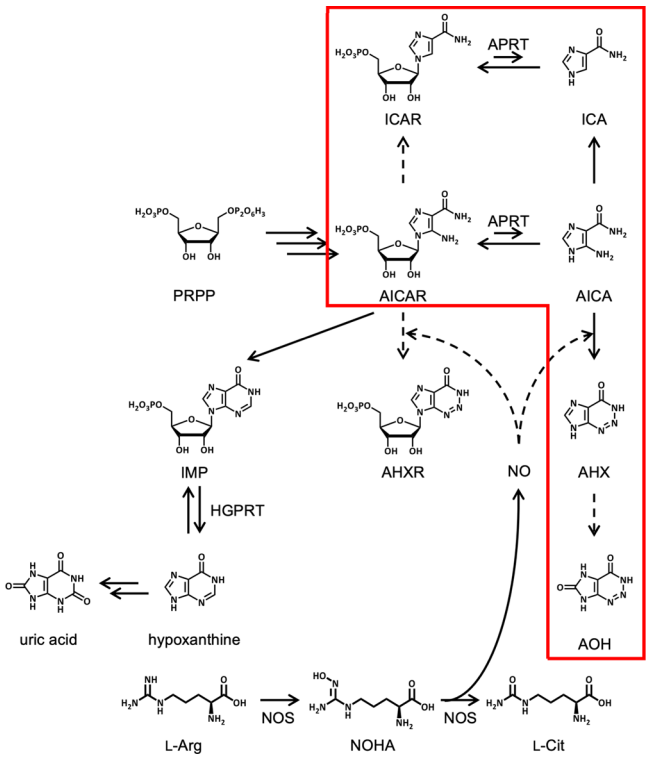


**Figure 1.** Fairy chemicals' (FCs') biosynthetic pathway in *L. sordida*. The three consecutive arrows represent multistage enzyme reactions. The routes indicated by solid arrows were already clarified, and those indicated by dashed arrows are speculated pathways. The endogenous existence of the compounds in the red frame has been reported by ref 16. PRPP, phosphoribosyl pyrophosphate.

discovered that the 1,2,3-triazine in 2-azahypoxanthine is formed from the reaction of 5-aminoimidazole-4-carboxamide with $N_2O_3$ and $NO^+$ in *L. sordida*. $NO^+$ itself is spontaneously derived from nitrogen oxide (NO) that is produced by NO synthase (NOS).[18] Generally, NOSs catalyze two-step oxidation reactions of L-Arg to generate L-Cit and NO via $N^G$-hydroxy-L-Arg (NOHA) as an intermediate.[18,19] Of the eight NOS genes in *L. sordida*, we found that recombinant NOS2 and NOS8 proteins produce NO from NOHA in the presence of hydrogen peroxide ($H_2O_2$).[18,20] The 1,2,3-triazine moiety can also be formed in 5-aminoimidazole-4-carboxamide-1-$\beta$-D-ribofuranosyl 5′-monophosphate through reaction with NOS-derived NO, producing 2-azahypoxanthine-ribonucleotide (AHXR). This raises the possibility that 2-azahypoxanthine could be produced from 2-azahypoxanthine-ribonucleotide through removal of the phosphoribose group, similar to the conversion of 5-aminoimidazole-4-carboxamide-1-$\beta$-D-ribofuranosyl 5′-monophosphate to 5-aminoimidazole-4-carboxamide.[18]

In addition, it has been reported that a recombinant adenine phosphoribosyltransferase from *L. sordida* (rAPRT) catalyzes reversible interconversion between 5-aminoimidazole-4-carboxamide-1-$\beta$-D-ribofuranosyl 5′-monophosphate and 5-aminoimidazole-4-carboxamide as well as between imidazole-4-carboxamide-ribonucleotide (imidazole-4-carboxamide-ribonucleotide) and imidazole-4-carboxamide (Figure 1). By contrast, rAPRT against 2-azahypoxanthine or 2-aza-8-oxohypoxanthine showed no activity.[16] Therefore, it is not known whether or how 2-azahypoxanthine and 2-aza-8-oxohypoxanthine might be directly interconverted with ribonucleotide forms. We hypothesized that a hypoxanthine-guanine phosphoribosyltransferase (HGPRT) that is present in *L. sordida* may carry out this role.[21] HGPRT is an enzyme that recognizes compounds having purine-like skeletons as substrates and catalyzes the reversible reactions between hypoxanthine and inosine monophosphate (IMP), guanine and guanosine monophosphate (GMP), and xanthine and xanthosine monophosphate (XMP).[22−26]

To characterize genes that may be involved in 2-azahypoxanthine biosynthesis and metabolism, we performed differential gene expression analysis of *L. sordida* cultures with high and low levels of 2-azahypoxanthine. In addition, we investigated the biochemical activities of heterologously expressed NOS5 and HGPRT proteins from *L. sordida* to determine whether they participate in FC metabolism.

## RESULTS AND DISCUSSION

We reasoned that comparisons of gene expression between mycelial cultures with high and low abundance of 2-azahypoxanthine may reveal transcriptional changes that influence 2-azahypoxanthine metabolism. Therefore, we quantified the amount of 2-azahypoxanthine present in *L. sordida* cultures and culture medium over time by UPLC. The maximum amount of 2-azahypoxanthine was 918.8 $\mu$mol/mg mycelia (dry weight) on day 3, and the minimum was 113.6 $\mu$mol/mg mycelia (dry weight) on day 21 (Figure 2). This led us to examine gene expression profiles with RNA-seq and RT-qPCR (reverse transcription quantitative PCR) in cultures grown for 3 and 21 days.

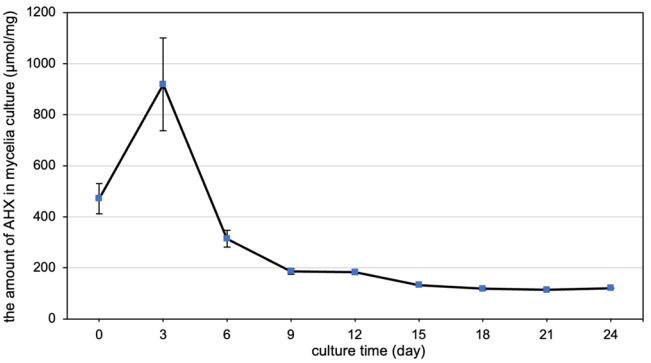


**Figure 2.** Time course of 2-azahypoxanthine (AHX) production in *L. sordida*. The fungus was liquid-cultured for 24 days and was sampled every 3 days. Amount of 2-azahypoxanthine in culture per mycelial weight (dry weight; mg) was quantified by UPLC. Error bar indicates standard deviation of five biological replicates.

Since 2-azahypoxanthine is made via 5-aminoimidazole-4-carboxamide-1-$\beta$-D-ribofuranosyl 5′-monophosphate, we first examined the expression of genes known to be involved in 5-aminoimidazole-4-carboxamide-1-$\beta$-D-ribofuranosyl 5′-monophosphate biosynthesis from the purine and histidine metabolic pathways.[17] In the purine metabolic pathway, adenylosuccinate lyase gene (accession no. GKV58048.1) transcript abundance was higher on day 3 of culturing, when the 2-azahypoxanthine level was highest, than day 21 (Figure 3A,B and Table S1). In the histidine metabolic pathway, the expression level of the imidazoleglycerol phosphate synthase gene (accession no. GKV58043.1) was also significantly increased on day 3 versus 21 according to RT-qPCR measurements (Figure 3B). This suggested that increased


https://doi.org/10.1021/acs.jnatprod.2c00789
J. Nat. Prod. XXXX, XXX, XXX−XXX

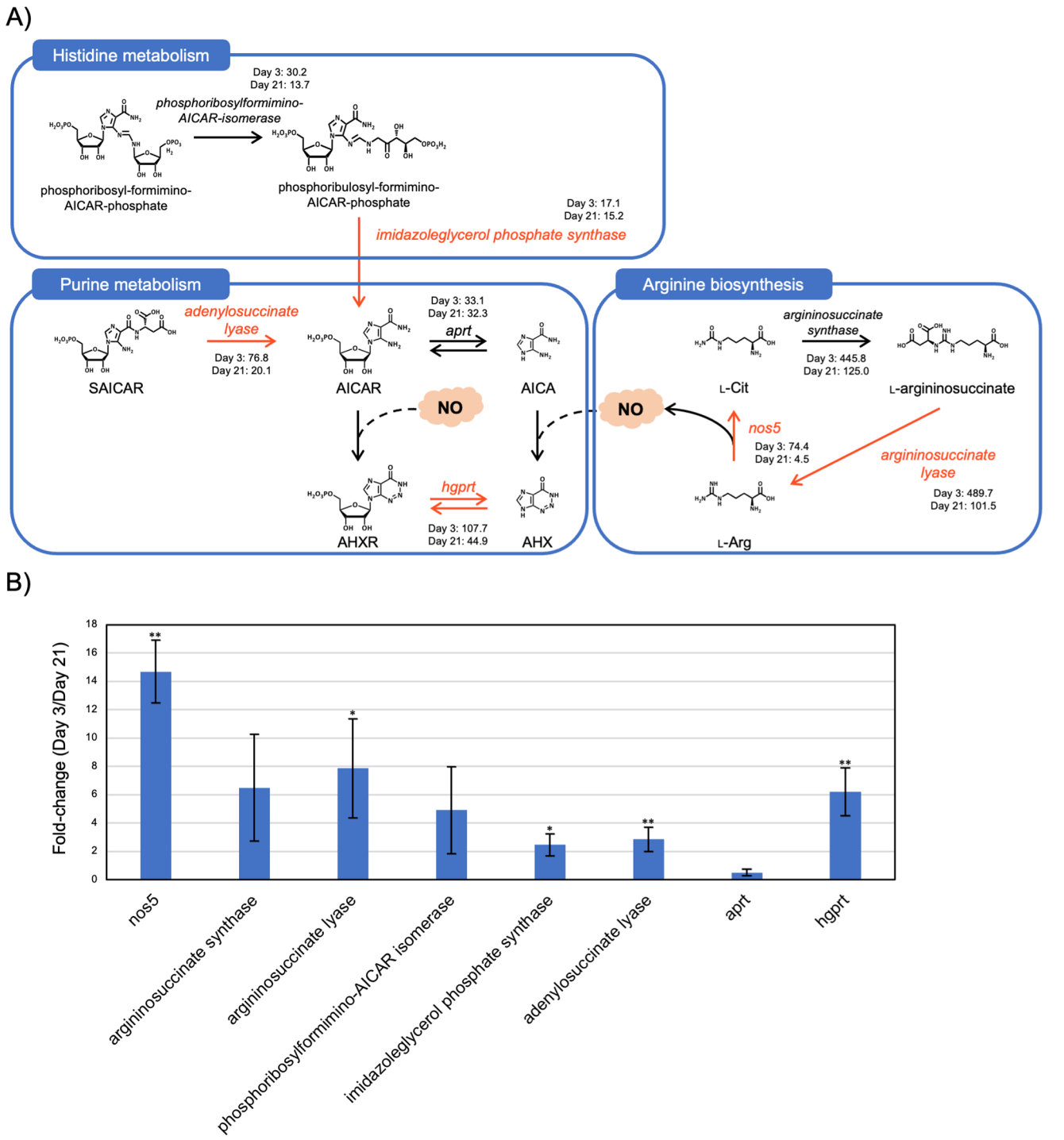


**Figure 3.** Target genes involved in 2-azahypoxanthine (AHX) production. (A) The biosynthetic and metabolic pathway of 2-azahypoxanthine predicted by gene expression profiling. The genes shown in orange were found to be highly expressed by RNA-seq and RT-qPCR analysis when the 2-azahypoxanthine level was high. The numbers near each enzyme names are the TPM values on day 3 and day 21. (B) Difference of relative expression of the genes evaluated by RT-qPCR between day 3 and day 21. The *actin* gene was used for the normalization of each gene expression. Error bar indicates standard deviation of five biological replicates. $*P < 0.05$ and $**P < 0.01$ indicate significant differences in two-tailed Student's *t*-tests.

expression of 5-aminoimidazole-4-carboxamide-1-$\beta$-D-ribofuranosyl 5′-monophosphate biosynthetic genes could promote the biosynthesis of 2-azahypoxanthine.

To identify significant changes in the gene expression at the time when 2-azahypoxanthine content was the highest (day 3) and lowest (day 21), gene ontology (GO) enrichment analysis was performed by parametric analysis of gene set enrichment (PAGE) based on the $\log_2$ fold-change (logFC).[27] On day 3, PAGE detected overrepresentations of 21 GO terms, including 8 biological processes, 4 cellular components, and 9 molecular functions with FDR < 0.05 (Supplementary Table S2). The GO terms "nucleoside metabolic process" and "purine nucleotide biosynthetic process" were also significantly overrepresented on day 3. Addition of 5-aminoimidazole-4-


https://doi.org/10.1021/acs.jnatprod.2c00789
J. Nat. Prod. XXXX, XXX, XXX−XXX

carboxamide-1-β-D-ribofuranosyl 5′-monophosphate during liquid culture of *L. sordida* enhances the expression of *aprt* (accession no. BAU71516.1).[16] Therefore, we predicted that *aprt* expression would be highest when 2-azahypoxanthine content was highest in this analysis as well. However, the expression level of *aprt* did not change (day 3: TPM = 33.1, day 21: TPM = 32.3) (Figure 3 and Table S1). Interestingly, the expression level of another phosphoribosyltransferase, *hgprt* (accession no. GKV58055.1), was significantly increased on day 3 compared to day 21 (day 3: TPM = 107.7, day 21: TPM = 44.9), suggesting that it may be involved in 2-azahypoxanthine biosynthesis (Figures 3A,B and Table S1).

2-Azahypoxanthine content in *L. sordida* is stimulated by addition of L-Arg to the culture medium.[18] Previously, this led us to hypothesize that NOS in *L. sordida* generates a nitrogen donor from L-Arg and the donor attacks 5-aminoimidazole-4-carboxamide to form 2-azahypoxanthine. Among the eight NOS genes in *L. sordida*, only *nos4* encodes all four functional domains that are typically found in NOS proteins, nitric oxide synthase, oxygenase domain (NO_synthase), flavodoxin_1, FAD_binding_1, and NAD_binding_1. On the hand, the other NOS proteins in *L. sordida* have a poorly conserved domain organization.[18] However, the expression level of *nos4* (accession no. GHP15259.1) was the lowest among the eight NOS genes. Phylogenetic analysis showed that NOS3 (accession no. GHP15258.1), NOS5 (accession no. GHP15260.1), NOS6 (accession no. GHP15261.1), and NOS7 (accession no. GHP15262.1) formed a distinct lineage group from the more highly expressed genes of NOS1 (accession no. GHP15256.1), NOS2 (accession no. GHP15257.1), and NOS8 (accession no. GHP15263.1). All proteins have only the NO_synthase among the four functional domains.[18]

We compared the expression levels of the eight *nos* genes in *L. sordida*. Expression of *nos5* was higher on day 3 of culturing than day 21 (day 3: TPM = 74.4, day 21: TPM = 4.5, Supplementary Table S1). By contrast, the expression levels of the other seven *nos* genes were not significantly different on days 3 and 21. In the arginine biosynthesis pathway, *argininosuccinate lyase* (accession no. GKV58042.1) was also highly expressed on day 3, suggesting increased abundance of the source of NO (Figure 3A and B). RT-qPCR analysis showed consistent results with the RNA-seq data for these genes (Figure 3B and Table S1).

To investigate which *nos* gene(s) is most likely to be involved in 2-azahypoxanthine biosynthesis, we examined the effect of L-Arg addition to *L. sordida* cultures on the expression of *nos1* to *nos8* by qRT-PCR. The transcript levels of *nos5*, *nos3*, and *nos7* were increased significantly by L-Arg treatment, with *nos5* showing the strongest response (Figure S2). Interestingly, *nos3* and *nos7* belong to the same evolutionary lineage as *nos5*.[18] These results suggest that NOS5 may be the main NOS involved in 2-azahypoxanthine biosynthesis. However, NOS5 also lacks a C-terminal reductase domain, like NOS2 and NOS8. This led us to hypothesize that NOS5 oxidizes NOHA to produce NO in the presence of an electron donor such as $H_2O_2$, similar to bacterial NOS enzymes.[18]

To test this idea, recombinant His-tagged NOS5 enzyme (rNOS5) was expressed in *E. coli*. The enzyme was refolded in the presence of hemin to yield the active form. We purified rNOS5 by Ni-affinity column chromatography, observing a single protein band in SDS-PAGE that agreed with its predicted molecular mass (92.5 kDa) (Figure S3). We then examined whether rNOS5 can produce NO from L-Arg and/or NOHA in the presence of $H_2O_2$. Neither rNOS2 nor rNOS8 showed activity with an L-Arg substrate, but were active with NOHA.[18] The activity of rNOS5 was also compared with those of rNOS2 and rNOS8. Similar to rNOS2 and rNOS8, rNOS5 did not show NO-producing activity with the L-Arg substrate (Figures 4 and S4). However, all three enzymes

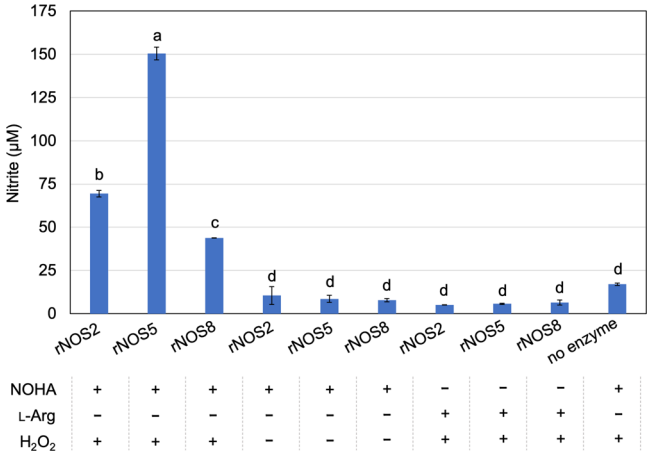


**Figure 4.** Activity of NOS enzymes against NOHA. Nitrite derived from NO was quantified by Griess reagent. Results are means ± standard errors ($n$ = 3). Bars represent means ± 95% confidence intervals. Different letters indicate statistical significance of difference in the Tukey−Kramer HSD test ($P$ < 0.001).

produced NO from a NOHA substrate. This activity was $H_2O_2$-dependent. We observed more than 2-fold higher NO production from rNOS5 than from rNOS2 or rNOS8 (Figures 4 and S4). Altogether, the expression pattern and enzymatic activity of *nos5* suggest that it is a key gene for 2-azahypoxanthine biosynthesis in *L. sordida*.

We previously observed that NO produced by rNOS2 converts 5-aminoimidazole-4-carboxamide-1-β-D-ribofuranosyl 5′-monophosphate to 2-azahypoxanthine-ribonucleotide *in vitro*.[18] As discussed above, we also hypothesized that HGPRT might catalyze a reversible reaction between 2-azahypoxanthine and 2-azahypoxanthine-ribonucleotide. Either mechanism could be expected to produce 2-azahypoxanthine-ribonucleotide in *L. sordida*, but 2-azahypoxanthine-ribonucleotide has not been detected *in vivo*. As mentioned above, the time course of 2-azahypoxanthine production in the whole culture (both the culture broth and mycelia) was analyzed, and the maximum production of it was on day 3 (Figure 2). 2-Azahypoxanthine-ribonucleotide was not detected in the broth. Therefore, we examined the time course of 2-azahypoxanthine-ribonucleotide production in the mycelia using chemically synthetic 2-azahypoxanthine-ribonucleotide as a standard.[28] As a result, 2-azahypoxanthine-ribonucleotide was not detected in the early stage of the culture, reaching the maximum on day 21 (Figure S5). These results suggest that HGPRT mainly plays a role in the reaction from 2-azahypoxanthine to 2-azahypoxanthine-ribonucleotide in the mycelia. This is the first reported detection of endogenous 2-azahypoxanthine-ribonucleotide (Figure 5).

To elucidate the hypothesized role of HGPRT, we heterologously overexpressed *hgprt* in *E. coli* and examined its function. Recombinant HGPRT (rHGPRT) was purified by Ni-affinity column chromatography and gave a single band on


https://doi.org/10.1021/acs.jnatprod.2c00789
J. Nat. Prod. XXXX, XXX, XXX−XXX

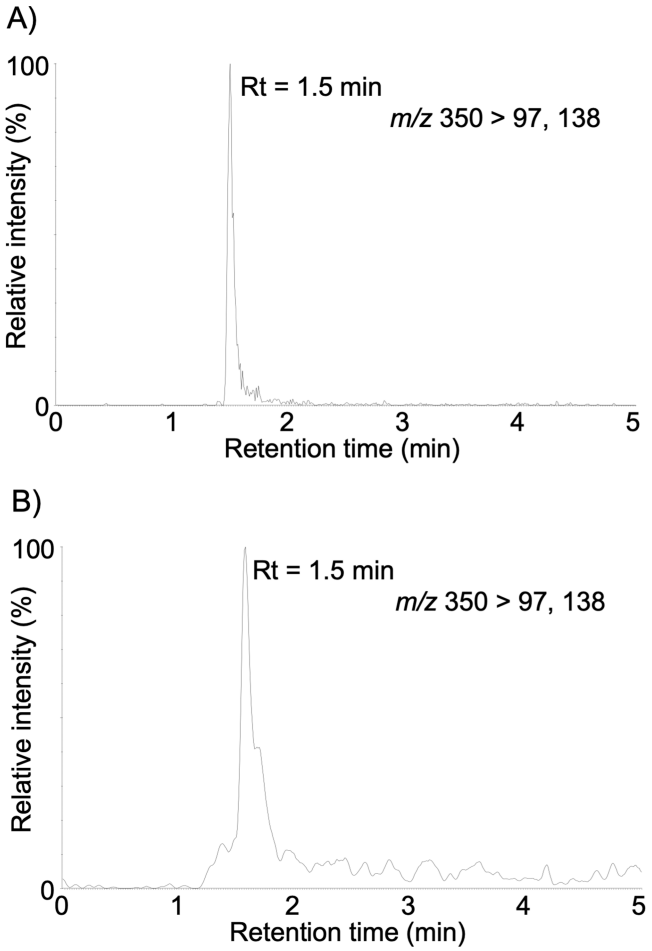


**Figure 5.** Detection of endogenous 2-azahypoxanthine-ribonucleotide in *L. sordida* mycelia on day 21 by LC-MS/MS. 2-Azahypoxanthine-ribonucleotide was detected in the positive ion mode. LC-MS/MS chromatograms indicate multiple reaction monitoring for (A) authentic 2-azahypoxanthine-ribonucleotide and (B) endogenous 2-azahypoxanthine-ribonucleotide in the sample. Rt, retention time.

SDS-PAGE consistent with its predicted molecular weight of 25.8 kDa (Figure S6). We tested rHGPRT for *in vitro* phosphoribosylation activity against hypoxanthine, 5-aminoimidazole-4-carboxamide, 2-azahypoxanthine, imidazole-4-carboxamide, and 2-aza-8-oxohypoxanthine. Hypoxanthine, 2-azahypoxanthine, imidazole-4-carboxamide, and 2-aza-8-oxohypoxanthine were converted to the corresponding mononucleotides, IMP, 2-azahypoxanthine-ribonucleotide, imidazole-4-carboxamide-ribonucleotide, and 2-aza-8-oxohypoxanthine-ribonucleotide (AOHR), respectively (Figure 6). Hypoxanthine was the most efficiently converted substrate for the enzyme, followed by 2-azahypoxanthine and 2-aza-8-oxohypoxanthine (Figure S7A and B). In contrast, rHGPRT activity against imidazole-4-carboxamide was very low, and no product was detected in the reaction using 5-aminoimidazole-4-carboxamide (Figures 6 and S7A). The dephosphoribosylation activity of rHGPRT was also examined using IMP, 5-aminoimidazole-4-carboxamide-1-$\beta$-D-ribofuranosyl 5′-monophosphate, 2-azahypoxanthine-ribonucleotide, and imidazole-4-carboxamide-ribonucleotide as substrates. 2-Aza-8-oxohypoxanthine-ribonucleotide has not yet been chemically synthesized and was not tested. Consistent with our hypothesis, rHGPRT converted 2-azahypoxanthine-ribonucleotide to 2-azahypoxanthine (Figures 6 and S7A). The reversible reaction between 2-azahypoxanthine and 2-azahypoxanthine-ribonucleotide was also confirmed by LC-MS/MS (Figure S8). In contrast, rHGPRT did not catalyze dephosphoribosylation of IMP, 5-aminoimidazole-4-carboxamide-1-$\beta$-D-ribofuranosyl 5′-monophosphate, or imidazole-4-carboxamide-ribonucleotide, even after incubating the reaction mixture for 24 h. The dephosphoribosylation activity of rHGPRT was considerably lower than its phosphoribosylation activity, as is the case for rAPRT.[16] Thus, HGPRT may primarily convert fairy chemicals to fairy chemical-ribotides *in vivo*, rather than generate fairy chemicals from fairy chemical-ribotides as expected. It remains to be determined whether fairy chemicals, their ribotide forms, or both, are the bioactive signals *in vivo*.

In conclusion, we have identified two genes that are likely involved in biosynthesis and metabolism of 2-azahypoxanthine in *L. sordida*. The expression patterns and *in vitro* activities of NOS5 and HGPRT suggest they are involved in the formation of 2-azahypoxanthine and 2-azahypoxanthine-ribonucleotide, which we have now detected *in vivo*. Our findings indicated that NOS5-derived NO may be involved in the biosynthesis of 2-azahypoxanthine, and HGPRT may regulate the amount of 2-azahypoxanthine by phosphoribosylation and dephosphoribosylation in *L. sordida*.

## EXPERIMENTAL SECTION

**General Experimental Procedures.** LC-MS/MS analyses were performed with a UPLC system (quatenary solvent manager, sample manager-FTN, PDA e$\lambda$ detector, Nihon Waters) coupled with a tandem Xevo TQ-S micro mass spectrometer (Nihon Waters). 5-Aminoimidazole-4-carboxamide and 5-aminoimidazole-4-carboxamide-1-$\beta$-D-ribofuranosyl 5′-monophosphate were purchased from Sigma-Aldrich Japan. 2-Azahypoxanthine, 2-aza-8-oxohypoxanthine, imidazole-4-carboxamide, 2-azahypoxanthine-ribonucleotide, and imidazole-4-carboxamide-ribonucleotide were synthesized according to the methods previously described.[28,29] All solvents used throughout the experiments were obtained from Kanto Chemical.

**Strain and Culture Condition.** *Lepista sordida* (NBRC112841) was originally collected from a lawn in Akita Prefecture, Japan. *L. sordida* was grown on a PDA plate (potato dextrose agar) at 25 °C for 3 weeks under dark conditions.

**Quantification of 2-azahypoxanthine by UPLC analysis.** The amount of 2-azahypoxanthine in the mycelia culture was determined by UPLC. Two disks of *L. sordida*, 8.5 mm diameter, were each placed into a 50 mL Erlenmeyer flask containing 10 mL of YG medium (1% D-glucose, 0.3% yeast extract, 0.05% $KH_2PO_4$, and 0.05% $Na_2HPO_4$, pH 5.5). The culture was performed at 120 rpm at 25 °C for 24 days in the dark, and the culture liquid was collected every 3 days. After cultivation, 20 mL of methanol and 300 $\mu$L of 1 mM allopurinol (internal standard for quantification) were added to all of the flasks to stop growth. The mycelia were homogenized by a Polytron PT 1200E homogenizer (Kinematica, Switzerland) for 1 min. Then 1 mL of each homogenized sample was dried by a centrifugal concentration device (CC-105, Tommy). The samples were redissolved in 100 $\mu$L of distilled water, and then subjected to UPLC analysis (column, CAPCELL PAK ADME, $\phi$ 2.1 × 250 mm, Osaka Soda; solvent, A: 10 mM ammonium formate, B: MeOH, 2% solvent B; flow rate, 0.4 mL/min; column oven, 40 °C, injection volume, 2 $\mu$L).

**RNA Extraction and Sequencing.** The mycelia were cultivated for 3 or 21 days as described above, and total RNA was extracted from biological triplicates of each culture stage. Samples were ground into a fine powder in liquid nitrogen, and total RNA was extracted using the TRIzol reagent (Thermo Fisher Scientific) according to the manufacturer's protocol. Total RNA was treated with DNase I (QIAGEN) and repurified using the RNeasy plant mini kit (QIAGEN). The quality of each total RNA was evaluated by


https://doi.org/10.1021/acs.jnatprod.2c00789
J. Nat. Prod. XXXX, XXX, XXX−XXX

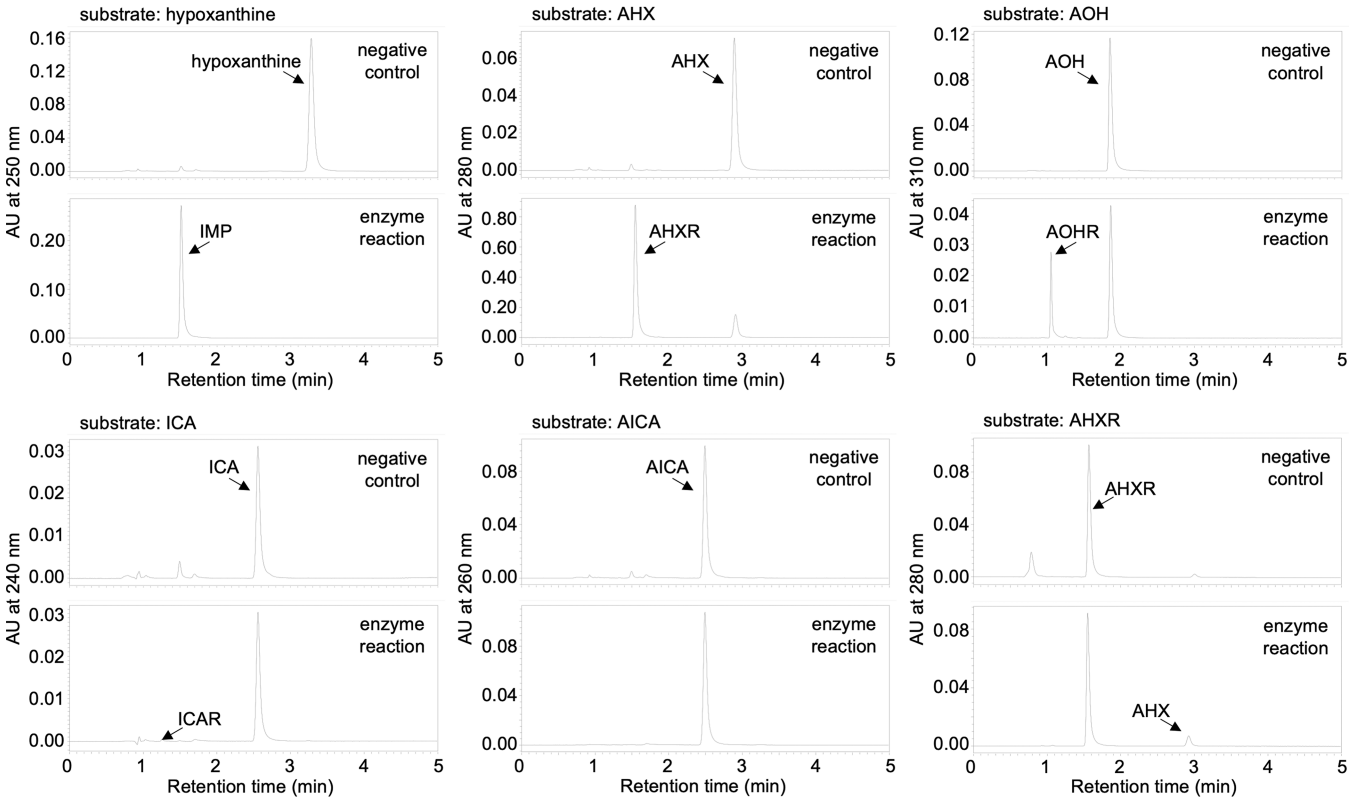


**Figure 6.** UPLC analysis of the products of phosphoribosylation and dephosphoribosylation by rHGPRT. Purified rHGPRT was incubated with each substrate in the presence of $Mg^{2+}$ and phosphoribosyl pyrophosphate (PRPP) or pyrophosphate at 37 °C for 1 h. Boiled enzyme was used for the negative control.

measuring the optical density using a Nanodrop ONE spectrophotometer (Thermo Scientific). The RNA integrity number was determined by an Agilent 2100 bioanalyzer (Agilent Technologies) and an Agilent RNA 1000 nano kit (Agilent Technologies). The RNA degradation and the contamination of genomic DNA were also checked by using 2% agarose gel electrophoresis. A cDNA library from the purified total RNA was prepared using a Kapa Stranded mRNA-Seq kit with Kapa mRNA capture beads (KAPA Biosystems). The average library length was confirmed using an Agilent 2100 bioanalyzer (Agilent Technologies), and absolute quantification was performed using the Kapa library quantification kit (KAPA Biosystems) according to the instruction manuals. The cDNA libraries were then sequenced (2 × 76 bp) on a MiSeq instrument at the Center for Bioscience Research and Education, Utsunomiya University, Japan.

**Differential Gene Expression Analysis and GO Enrichment Analysis.** The raw reads were filtered using Trimmomatic v. 0.36[30] with the following parameters: CROP: 75, SLIDINGWINDOW: 4:15, and MINLEN: 50. The filtered 24,963,852 read pairs totaling 3.73 Gb were aligned to the reference genome sequence of *L. sordida* NBRC 112841 (GenBank accession number BIMQ00000000) using HISAT2 v. 2.2.0[31] with minimum and maximum intron lengths of 20 and 1000 bp, respectively. Read counts were calculated from bam files using featureCounts v. 2.0.0[32] and normalized with transcripts per million (TPM) values and scaling factors for the library sizes using a trimmed mean of M-values method.[33] Differentially expressed genes (DEGs) between samples cultivated for 3 and 21 days were identified using the likelihood-ratio test implemented in the edgeR package v. 3.16.5[34] and defined by the $\log_2$ fold-change (logFC) > 1 and logFC < −1 with a false discovery rate (FDR) < 0.01. To identify significantly changed biological features in the sample with higher levels of 2-azahypoxanthine, we performed GO enrichment analysis by PAGE.[35] First, GO terms were assigned to *L. sordida* proteome using InterProScan-5.45-80.0[36] with a goterms option. Over- and under-represented GO terms were tested by PAGE based on the logFC values between samples cultivated on day 3 and 21 with FDR < 0.05.

**Quantitative Reverse Transcription PCR Analysis.** For comparison of high and low 2-azahypoxanthine content, *L. sordida* mycelia cultured for 3 or 21 days were used. For comparison of *nos1* to *-8* expression levels, the mycelia incorporating 1 mM L-Arg or sterile water were used. The culture method was as described above. After one week of preculture, L-Arg or sterile water was added to the culture for 3 days under dark conditions. Total RNA was isolated in the same way as in the RNA-seq experiments. A cDNA was reverse-transcribed from 500 ng of total RNA with PrimeScript RT reagent kit Perfect Real Time (TaKaRa Bio). To analyze gene expression in *L. sordida*, samples were prepared using PrimeScript RT reagent kit (Perfect Real Time) (TaKaRa). Single-stranded cDNAs were used as templates for quantitative reverse transcription PCR (RT-qPCR). RT-qPCR was performed using LightCycler 480 System II (Roche). *L. sordida actin* gene was used for the normalization of gene expression levels. The sequences of primers designed for this study are listed in Supplementary Table 3. The thermocycling condition included an initial denaturation step at 95 °C for 10 min, followed by 45 cycles of denaturation at 95 °C for 10 s, primer annealing at 64 °C for 10 s, and extension at 72 °C for 15 s using FastStart essential DNA green master (Roche). Relative quantitation using the comparative $C_t$ method was calculated as $\Delta\Delta C_t = (\Delta C_{t,target} - \Delta C_{t,control})_{fermenting\ conditions} - (\Delta C_{t,target} - \Delta C_{t,control})_{nonfermenting\ conditions}$.

**Detection of Endogenous 2-Azahypoxanthine-ribonucleotide in *L. sordida* Mycelia.** *L. sordida* mycelia were cultured for 21 days, freeze-dried, and stored at −80 °C until extraction. The mycelia (20 mg) were extracted according to the high-sensitivity detection method for purine metabolites.[13] Each sample was dissolved in 150 μL of 80% MeCN and subjected to LC-MS/MS analysis. The column and solvent conditions used for this analysis were the same as for the UPLC analysis. For 2-azahypoxanthine-ribonucleotide detection, MS analysis was performed in the positive mode with the following source parameters: cone voltage, 16 V; collision energy, 22 ($m/z$ 350 > 97)


https://doi.org/10.1021/acs.jnatprod.2c00789
J. Nat. Prod. XXXX, XXX, XXX−XXX

and 16 V ($m/z$ 350 > 138). The following source parameters were common to all the compounds: capillary voltage, 3.0 kV; desolvation temperature, 500 °C; desolvation gas flow, 1000 L/h; cone gas flow, 50 L/h.

**Heterologous Expression of Recombinant NOS5 and HGPRT in *E. coli*.** *L. sordida* mycelia were frozen in liquid nitrogen and ground into a powder. A cDNA was prepared from the resulting mycelial powder by the same method used to obtain RT-qPCR samples. Full-length cDNAs of the *nos5* and *hgprt* were amplified by RT-PCR using PrimeSTAR Max DNA polymerase (TaKaRa Bio). All primers used in this experiment are listed in Table S3. The reaction mixture (10 μL) contained 50 ng of total cDNA, 5 μL of PrimeSTAR Max DNA polymerase, and 0.5 μM of each primer. Cycling conditions were set as follows: preincubation, 1 cycle of 94 °C for 2 min; amplification, 35 cycles of 98 °C for 10 s (for *nos5*) or 15 s (for *hgprt*), 60 °C for 15 s (for *nos5*) or 61 °C for 30 s (for *hgprt*), and 72 °C for 30 s (for *nos5*) or 72 °C for 10 s (for *hgprt*). The amplified PCR products were ligated into the pET21c(+) expression vector (Sigma-Aldrich Japan) between *Nde*I and *Xho*I sites using Gibson assembly master mix (New England BioLabs Japan) (for *nos5*) or pColdI expression vector (TaKaRa Bio) linearized by NdeI and *Bam*HI cleavage (for *hgprt*), followed by transformation into *E. coli* DH5α competent cells (Nippon Gene). The plasmids (pET21c(+)-*nos5*, pColdI-*hgprt*) were extracted with the HiYield plasmid mini kit (RBC Bioscience). The authenticity of the resulting plasmid DNAs was confirmed by PCR amplification and sequencing, and then the plasmids were transformed into *E. coli* SHuffle T7 express (New England BioLabs Japan) or *E. coli* BL21-CodonPlus (DE3)-RIPL competent cells (Agilent Technologies Japan). For expression of NOS5, the culture (4 mL) was added into lysogeny broth (LB) medium containing ampicillin, and the culture (1 L) was incubated (37 °C, 150 rpm) until the $OD_{600}$ reached 0.3. 5-Aminolevulinic acid (Wako Pure Chemical) (final 1 mM) and $FeSO_4 \cdot 7H_2O$ (final 100 mM) were added, and the culture was further incubated until the $OD_{600}$ reached 0.4 and then was cooled to 18 °C. Recombinant protein expression was induced by 1 mM isopropyl β-D-1-thiogalactopyranoside (IPTG), and the cells were cultured (18 °C, 125 rpm) for 24 h. For expression of HGPRT, the transformant was grown in 1 L of LB medium containing ampicillin at 37 °C until the $OD_{600}$ reached 0.4. After incubation at 4 °C for 30 min, rHGPRT was induced by 0.1 mM IPTG and the cells were cultured at 15 °C for at least 24 h. The cells were harvested by centrifugation and stored at −80 °C until protein extraction.

**Purification of rNOS5 and rHGPRT.** The cells were suspended in extraction buffer (20 mM Tris-HCl, pH 7.4, 500 mM NaCl, 10% glycerol, and 30 mM imidazole for rNOS5, or 100 mM Tris-HCl, pH 7.4, 100 mM NaCl, and 30 mM imidazole for rHGPRT). After lysis by sonication for 30 min on ice, the cell debris was removed by centrifugation. The supernatant was filtered using a membrane filter and subjected to Ni affinity column chromatography using HisTrap HP (GE Healthcare Japan). After washing the column with wash buffer (20 mM Tris-HCl, pH 7.4, 500 mM NaCl, 10% glycerol, and 50 mM imidazole for rNOS5, or 20 mM Tris-HCl, pH 7.4, 100 mM NaCl, and 30 mM imidazole for rHGPRT), 6× His-tagged proteins were eluted with elution buffer (20 mM Tris-HCl, pH 7.4, 500 mM NaCl, 10% glycerol, and 1 M imidazole for rNOS5, or 20 mM Tris-HCl, pH 7.4, 100 mM NaCl, and 1 M imidazole for rHGPRT) with a linear gradient (50 to 500 mM for rNOS5 or 0.03 to 1 M imidazole for rHGPRT). The eluted fractions of recombinant proteins were confirmed by 10% (for rNOS5) or 12.5% (for rHGPRT) SDS-PAGE with Coomassie brilliant blue staining and desalted against dialysis buffer (20 mM Tris-HCl, pH 7.4, 500 mM NaCl, and 10% glycerol) at 4 °C. After dialysis, the protein solutions were concentrated and replaced with enzyme buffer (100 mM Tris-HCl, pH 7.4, 100 mM NaCl, and 10% glycerol) using Amicon Ultra-0.5 mL 10K (Merck). The purified proteins' concentrations were quantified using the Pierce 660 nm protein assay reagent (Thermo Fisher Scientific) with BSA as a standard, and the enzymes were stored on ice until further used.

**Refolding of rNOS5 Protein.** *E. coli* cells were extracted using the same extraction method described above, and the cell debris was recovered by centrifugation. Based on the refolding methods of plant and fungal recombinant peroxidases, a refolding mixture (20 mL) containing 15 mg of protein, 3 M urea, 50 mM Tris-HCl (pH 9.5), 10% glycerol, 0.7 mM glutathione disulfide (Tokyo Chemical Industry), 0.2 mM glutathione (Tokyo Chemical Industry), and 10 μM hemin (Tokyo Chemical Industry) was prepared.[37−39] The mixture was incubated at 4 °C for 36 h and desalted against dialysis buffer (20 mM Tris-HCl, pH 7.4, 500 mM NaCl, and 10% glycerol). After dialysis, the filtered protein solution was purified as described above.

***In Vitro* Enzyme Assay of rNOS5.** The enzyme reaction mixture (30 mL) contained 5 μM rNOS5, 1 mM $N^G$-hydroxy-L-Arg (Sigma-Aldrich Japan) or L-Arg, 40 mM $H_2O_2$ (Wako Pure Chemical), and 50 mM HEPES-NaOH (pH 7.0).[20] The reaction was initiated by adding $H_2O_2$ and terminated with 20 mL of catalase (200 Units) (Wako Pure Chemical). The reaction mixture was incubated for 15 min at 30 °C. Nitrite was detected with Griess reagents (Cayman Chemical) containing sulfanilamide and *N*-(1-naphthyl)ethylenediamine, and absorbance was measured at 540 nm, using a Spark multimode microplate reader (Tecan).

***In Vitro* Enzyme Assays of rHGPRT.** For the phosphoribosylation activity, an enzyme reaction mixture (100 μL) containing 0.2 mM substrate (hypoxanthine, 5-aminoimidazole-4-carboxamide, 2-azahypoxanthine, imidazole-4-carboxamide, or 2-aza-8-oxohypoxanthine), 1 mM PRPP (Sigma-Aldrich Japan), 10 mM $MgCl_2 \cdot 6H_2O$, 20 mM Tris-HCl (pH 7.4), and 5 μM rHGPRT was prepared. For the dephosphoribosylation activity, the enzyme reaction mixture (100 μL) consisted of 0.2 mM substrate (IMP, 5-aminoimidazole-4-carboxamide-1-β-D-ribofuranosyl 5′-monophosphate, 2-azahypoxanthine-ribonucleotide, or imidazole-4-carboxamide-ribonucleotide), 1 mM sodium pyrophosphate decahydrate (Sigma-Aldrich Japan), 10 mM $MgCl_2 \cdot 6H_2O$, 20 mM Tris-HCl (pH 7.4), and 5 μM rHGPRT. The enzyme boiled for 10 min before the reaction was used as a negative control. The reaction mixture was preincubated at 37 °C for 5 min, and then the reaction was initiated by adding the enzyme solution. The reaction was terminated by boiling the mixture for 10 min, and then the mixture was centrifuged to precipitate proteins. Phosphorylation activity with hypoxanthine, 2-azahypoxanthine, and 2-aza-8-oxohypoxanthine was also tested at a substrate concentration of 600 μM. The enzyme reaction products in the supernatant were detected by UPLC analysis. The reversible reaction between 2-azahypoxanthine and 2-azahypoxanthine-ribonucleotide was also detected by LC-MS/MS. The column and solvent conditions used for this analysis were the same as for the UPLC analysis. For 2-azahypoxanthine detection, MS analysis was performed in the positive mode with the following source parameters: cone voltage, 6 V; collision energy, 12 ($m/z$ 138 > 55, 67). The other source parameters are as described above.

## ■ ASSOCIATED CONTENT

### Data Availability Statement

Raw reads for RNA-seq analyzed in this study have been deposited in the DDBJ Sequence Read Archive (DRA) under the accession numbers DRR377286 and DRR377287 for samples cultivated for 3 and 21 days, respectively.

### Supporting Information

The Supporting Information is available free of charge at https://pubs.acs.org/doi/10.1021/acs.jnatprod.2c00789.

> Chemical synthetic route of fairy chemicals, TPM value in MiSeq analysis, overrepresented GO terms when 2-azahypoxanthine level was high in *L. sordida*, the relative expression levels of *nos1* to *-8* in response to L-Arg feeding, SDS-PAGE of rNOS5 and rHGPRT, enzyme properties of rNOS5 and rHGPRT (PDF)



https://doi.org/10.1021/acs.jnatprod.2c00789
J. Nat. Prod. XXXX, XXX, XXX−XXX

## AUTHOR INFORMATION


### Corresponding Authors

**Jae-Hoon Choi** − *Graduate School of Science and Technology, Graduate School of Integrated Science and Technology, Faculty of Agriculture, Research Institute of Green Science and Technology, and Research Institute for Mushroom Science, Shizuoka University, Shizuoka 422-8529, Japan*; Phone: +81-54-238-3037; Email: choi.jaehoon@shizuoka.ac.jp

**Hirokazu Kawagishi** − *Faculty of Agriculture and Research Institute for Mushroom Science, Shizuoka University, Shizuoka 422-8529, Japan*; orcid.org/0000-0001-5782-4981; Phone: +81-54-238-4885; Email: kawagishi.hirokazu@shizuoka.ac.jp

### Authors

**Mihaya Kotajima** − *Graduate School of Science and Technology, Shizuoka University, Shizuoka 422-8529, Japan*

**Hyogo Suzuki** − *Graduate School of Integrated Science and Technology, Shizuoka University, Shizuoka 422-8529, Japan*

**Tomohiro Suzuki** − *Center for Bioscience Research and Education, Utsunomiya University, Utsunomiya, Tochigi 321-8505, Japan; Research Institute for Mushroom Science, Shizuoka University, Shizuoka 422-8529, Japan*; orcid.org/0000-0002-2444-5288

**Jing Wu** − *Faculty of Agriculture and Research Institute for Mushroom Science, Shizuoka University, Shizuoka 422-8529, Japan*

**Hirofumi Hirai** − *Graduate School of Science and Technology, Graduate School of Integrated Science and Technology, Faculty of Agriculture, Research Institute of Green Science and Technology, and Research Institute for Mushroom Science, Shizuoka University, Shizuoka 422-8529, Japan*

**David C. Nelson** − *Department of Botany and Plant Sciences, University of California, Riverside, California 92521, United States*

**Hitoshi Ouchi** − *School of Pharmaceutical Sciences, University of Shizuoka, Shizuoka 422-8526, Japan*

**Makoto Inai** − *School of Pharmaceutical Sciences, University of Shizuoka, Shizuoka 422-8526, Japan*; orcid.org/0000-0001-7074-0520

**Hideo Dohra** − *Graduate School of Integrated Science and Technology, Research Institute of Green Science and Technology, and Research Institute for Mushroom Science, Shizuoka University, Shizuoka 422-8529, Japan*; orcid.org/0000-0002-3919-3538

Complete contact information is available at: https://pubs.acs.org/10.1021/acs.jnatprod.2c00789


### Author Contributions

H.K. conceived the project and designed outlines for most of the experiments. T.S. and H.D. participated in bioinformatics work. M.K. and H.S. performed the experiments. H.O. and M.I. synthesized authentic 2-azahypoxanthine-ribonucleotide. J.-H.C., J.W., H.H., and H.K. assisted with the experiments and contributed to discussions. M.K., J.-H.C., H.D., D.C.N., and H.K. wrote the manuscript.

### Notes

The authors declare no competing financial interest.

## ACKNOWLEDGMENTS

We thanked Dr. K. Okamoto (Ushio Chemix, Shizuoka, Japan) for providing authentic 2-azahypoxanthine and imidazole-4-carboxamide. This study was mainly supported by Grant-in Aid for Specially Promoted Research "Science of fairy chemicals and their application development" (JP20H05620) from JSPS to H.K. and was also partially supported by a grant from the Institute for Fermentation, Osaka, to J.H.C. This work was also partially supported by JST, ACT-X Grant Number JPMJAX2115, Japan, to J.W.

## REFERENCES


(1) Couch, H. B. *Diseases of Turfgrasses*, 3rd ed.; Krieger Pub Co., 1995; pp 181−186.

(2) Beard, J. B. *Turfgrass Science and Culture*; Pearson, 2000; pp 574−626

(3) Lawes, J. B.; Gilbert, J. H.; Warington, R. *Journal of the Chemical Society* **1883**, *43*, 208−223.

(4) Evershed, H. *Nature* **1884**, *29*, 384−385.

(5) Shantz, H. L.; Piemeisel, R. L. *J. Agric. Res* **1917**, *11*, 191−245.

(6) Kawagishi, H. *Proc. Japan Acad. Ser. B* **2019**, *95*, 29−38.

(7) Kawagishi, H. *Biosci. Biotechnol. Biochem.* **2018**, *82*, 752−758.

(8) Terashima, Y.; Fukiharu, T.; Fujiie, A. *Mycoscience* **2004**, *45*, 251−260.

(9) Choi, J.-H.; Fushimi, K.; Abe, N.; Tanaka, H.; Maeda, S.; Morita, A.; Hara, M.; Motohashi, R.; Matsunaga, J.; Eguchi, Y.; Ishigaki, N.; Hashizume, D.; Koshino, H.; Kawagishi, H. *ChemBioChem* **2010**, *11*, 1373−1377.

(10) Choi, J.-H.; Abe, N.; Tanaka, H.; Fushimi, K.; Nishina, Y.; Morita, A.; Kiriiwa, Y.; Motohashi, R.; Hashizume, D.; Koshino, H.; Kawagishi, H. *J. Agric. Food Chem.* **2010**, *58*, 9956−9959.

(11) Choi, J.-H.; Ohnishi, T.; Yamakawa, Y.; Takeda, S.; Sekiguchi, S.; Maruyama, W.; Yamashita, K.; Suzuki, T.; Morita, A.; Ikka, T.; Motohashi, R.; Kiriiwa, Y.; Tobina, H.; Asai, T.; Tokuyama, S.; Hirai, H.; Yasuda, N.; Noguchi, K.; Asakawa, T.; Sugiyama, S.; Kan, T.; Kawagishi, H. *Angew. Chemie Int. Ed.* **2014**, *53*, 1552−1555.

(12) Mitchinson, A. *Nature* **2014**, *505*, 298.

(13) Takemura, H.; Choi, J.-H.; Matsuzaki, N.; Taniguchi, Y.; Wu, J.; Hirai, H.; Motohashi, R.; Asakawa, T.; Ikeuchi, K.; Inai, M.; Kan, T.; Kawagishi, H. *Sci. Rep.* **2019**, *9*, 9989.

(14) Tobina, H.; Choi, J.-H.; Asai, T.; Kiriiwa, Y.; Asakawa, T.; Kan, T.; Morita, A.; Kawagishi, H. *Field Crop Res.* **2014**, *162*, 6−11.

(15) Asai, T.; Choi, J.-H.; Ikka, T.; Fushimi, K.; Abe, N.; Tanaka, H.; Yamakawa, Y.; Kobori, H.; Kiriiwa, Y.; Motohashi, R.; Deo, V. K.; Asakawa, T.; Kan, T.; Morita, A.; Kawagishi, H. *Jpn. Agric. Res. Quart.* **2015**, *49*, 45−49.

(16) Ito, A.; Choi, J.-H.; Takemura, T.; Kotajima, M.; Wu, J.; Tokuyama, S.; Hirai, H.; Asakawa, T.; Ouchi, H.; Inai, M.; Kan, T.; Kawagishi, H. *J. Nat. Prod.* **2020**, *83*, 2469−2476.

(17) Suzuki, T.; Yamamoto, N.; Choi, J.-H.; Takano, T.; Sasaki, Y.; Terashima, Y.; Ito, A.; Dohra, H.; Hirai, H.; Nakamura, Y.; Yano, K.; Kawagishi, H. *Sci. Rep.* **2016**, *6*, 39087.

(18) Ito, A.; Choi, J.-H.; Yokoyama-Maruyam, W.; Kotajima, M.; Wu, J.; Suzuki, T.; Terashima, Y.; Suzuki, H.; Hirai, H.; Nelson, C. D.; Tsunematsu, Y.; Watanabe, K.; Asakawa, T.; Ouchi, H.; Inai, M.; Dohra, H.; Kawagishi, H. *Org. Biomol. Chem.* **2022**, *20*, 2636−2642.

(19) Wang, Z.-Q.; Lawson, J. R.; Buddha, R. M.; Wei, C.-C.; Crane, R. B.; Munro, W. A.; Stuehr, J. D. *J. Biol. Chem.* **2007**, *282*, 2196−2202.

(20) Zhao, G.; Guo, Y.-Y.; Yao, S.; Shi, X.; Lv, L.; Du, Y.-L. *Nat. Commun.* **2020**, *11*, 1614.

(21) Takano, T.; Yamamoto, N.; Suzuki, T.; Dohra, H.; Choi, J.-H.; Terashima, Y.; Yokoyama, K.; Kawagishi, H.; Yano, K. *Sci. Rep.* **2019**, *9*, 5888.

(22) Craig, S. P., III; Eakin, E. A. *J. Biol. Chem.* **2000**, *275*, 20231−20234.




https://doi.org/10.1021/acs.jnatprod.2c00789
J. Nat. Prod. XXXX, XXX, XXX−XXX

(23) Ashihara, H.; Stasolla, C.; Fujimura, T.; Crozier, A. *Phytochemistry* **2018**, *147*, 89−124.
(24) Arnold, W. J.; Kelley, W. N. *J. Biol. Chem.* **1971**, *246*, 7398−7406.
(25) Liu, X.; Qian, W.; Liu, X.; Qin, H.; Wang, D. *New Phytol.* **2007**, *175*, 448−461.
(26) Zhang, N.; Gong, X.; Lu, M.; Chen, X.; Qin, X.; Ge, H. *J. Struct. Biol.* **2016**, *194*, 311−316.
(27) Robinson, M. D.; McCarthy, D. J.; Smyth, G. K. *Bioinformatics* **2010**, *26*, 139−140.
(28) Ikeuchi, K.; Fujii, R.; Sugiyama, S.; Asakawa, T.; Inai, M.; Hamashima, Y.; Choi, J.-H.; Suzuki, T.; Kawagishi, H.; Kan, T. *Org. Biomol. Chem.* **2014**, *12*, 3813−3815.
(29) Choi, J.-H.; Matsuzaki, N.; Wu, J.; Kotajima, M.; Hirai, H.; Kondo, M.; Asakawa, T.; Inai, M.; Ouchi, H.; Kan, T.; Kawagishi, H. *Org. Lett.* **2019**, *21*, 7841−7845.
(30) Bolger, A. M.; Lohse, M.; Usadel, B. *Bioinformatics* **2014**, *30*, 2114−2120.
(31) Kim, D.; Paggi, J. M.; Park, C.; Bennett, C.; Salzberg, S. L. *Nat. Biotechnol.* **2019**, *37*, 907.
(32) Liao, Y.; Smyth, G. K.; Shi, W. *Bioinformatics* **2014**, *30*, 923−930.
(33) Robinson, M. D.; Oshlack, A. *Genome Biol.* **2010**, *11*, R25.
(34) Robinson, M. D.; McCarthy, D. J.; Smyth, G. K. *Bioinformatics* **2010**, *26*, 139−140.
(35) Kim, S. Y.; Volsky, D. J. *BMC Bioinformatics* **2005**, *6*, 144.
(36) Jones, P.; Binns, D.; Chang, H.-Y.; Fraser, M.; Li, W.; McAnulla, C.; McWilliam, H.; Maslen, J.; Mitchell, A.; Nuka, G.; Pesseat, S.; Quinn, F. A.; Sangrador-Vegas, A.; Scheremetjew, M.; Yong, S.-Y.; Lopez, R.; Hunter, S. *Bioinformatics* **2014**, *30*, 1236−1240.
(37) Smith, T. A.; Santama, N.; Dacey, S.; Edwards, M.; Bray, C. R.; Thorneley, N. R.; Burke, F. J. *J. Biol. Chem.* **1990**, *265*, 13335−13343.
(38) Miki, Y.; Morales, M.; Ruiz-Dueñas, J. F.; Martínez, J. M.; Wariishi, H.; Martínez, T. A. *Protein Expr. Purif.* **2009**, *68*, 208−214.
(39) Shigeto, J.; Itoh, Y.; Tsutsumi, Y.; Kondo, R. *FEBS J.* **2012**, *279*, 348−357.


https://doi.org/10.1021/acs.jnatprod.2c00789
*J. Nat. Prod.* XXXX, XXX, XXX−XXX